Resonance scattering of positronium atoms by nitrogen molecules

R. S. Wilde[1] and I. I. Fabrikant[2]

[1]*Department of Natural Sciences, Oregon Institute of Technology,*

Klamath Falls, Oregon 97601, USA

[2]*Department of Physics and Astronomy,*

University of Nebraska, Lincoln, Nebraska 68588-0299, USA

(Dated: June 10, 2020)

Abstract

We study theoretically the resonance scattering of positronium (Ps) atoms by nitrogen molecules and compare it with resonance $e-N_2$ scattering in the Π_g symmetry. The velocity positions of the $Ps-N_2$ resonances in Σ_u, Π_u, and Δ_g symmetries are very close to the velocity position of the $e-N_2$ resonance which leads to the total $Ps-N_2$ cross section being very similar to the $e-N_2$ cross section when both are plotted as functions of the projectile velocity. However, in the $Ps-N_2$ case the resonances are much wider and their positions vary much slower with increasing internuclear separation than in the $e-N_2$ case. This makes the Ps-impact vibrational excitation cross section much smaller than the electron-impact vibrational excitation cross section, and no boomerang oscillations are observed in $Ps-N_2$ scattering. We analyze the role of the static potential in the $e-N_2$ case and compare exchange potentials for $e-N_2$ and $Ps-N_2$ interactions. This analysis allows us to explain the difference in the vibrational dynamics in these two cases.

PACS numbers:

1

I. INTRODUCTION

Theoretical treatment of positronium (Ps) collisions with neutral targets is very challenging, therefore until recently most efforts have been mostly exclusively directed towards studies of Ps collisions with atoms [1]. A few theoretical studies of Ps collisions with the H_2 molecule are available [2–5], and, to the best of our knowledge, only one theoretical calculation of $Ps-N_2$ collisions [6] exists. Interest in Ps collisions with neutral targets is in much extent due to an intriguing similarity between electron and Ps scattering [7–9] which was recently extended to resonant scattering in $Ps-N_2$ [9, 10] and $Ps-CO_2$ [8] collisions. In particular the very well-known resonance in $e-N_2$ scattering of the Π_g symmetry [11] looks very similar to the observed resonance in the $Ps-N_2$ scattering if cross sections for both processes are plotted as functions of the projectile velocity.

Resonances in electron-molecule collisions drive many inelastic processes, particularly vibrational excitation and dissociative electron attachment [12, 13]. Therefore, if similar resonances exist in Ps-molecule collisions, they can drive similar processes, particularly Ps-impact vibrational excitation and dissociative Ps attachment.

The Π_g resonance in $e-N_2$ scattering has been studied in many theoretical and experimental papers [11]. Theoretical papers on $e-N_2$ resonant scattering can be separated into two categories: calculations performed in the fixed-nuclei approximations [14–19] and calculations which account for vibrational motion [20–26]. In the second class of calculations a single resonance is split into series of peaks, so-called boomerang oscillations [21], which appear because the resonance lifetime is comparable with the vibrational period in N_2.

On the other hand, positron-nitrogen collisions were studied both experimentally [27] and theoretically [28]. Whereas no resonances are observed in this process, the total cross section becomes very large at low energies due to virtual Ps formation which is directly related to experiments on positron annihilation in positron collisions with neutral targets [29].

In our recent paper [6] we investigated $Ps-N_2$ collisions by employing model exchange and correlation potentials [30]. Interaction of Ps with electrons in the molecular target was described on the basis of the free-electron-gas (FEG) model with both electron and positron in the projectile Ps treated on equal footing. The interaction consists of two components, an exchange and correlation potential. Because of the presence of the positron in Ps, the exchange potential for the Ps-molecule interaction is quite different from that for the

electron-molecule interaction, as will be explicitly demonstrated in the present paper. The correlation potential turns asymptotically into the van der Waals interaction which is also very different from the polarization potential dominating the electron-molecule interaction. Resonances in three partial waves, Σ_u, Π_u, and Δ_g, have been found in [6]. They lead to two peaks in the scattering cross section as a function of energy whose positions are close to each other and close to the position of the experimentally observed peak [10]. Whereas there cannot be a direct connection between resonance symmetries in $e - N_2$ and $Ps-N_2$ collisions, a close similarity in the shape and the magnitude of the cross section is interesting and suggests a possible similarity in inelastic collisions.

The previous calculations [6] of $Ps-N_2$ scattering were done in the fixed-nuclei approximation. To calculate Ps-impact vibrational excitation cross sections we need to investigate first the dependence of the scattering matrices on the internuclear separation R. These calculations are discussed in Sec. II of the present paper. We find that for all three resonances their widths are large compared to the vibrational quantum $\hbar\omega$ in N_2. Therefore the boomerang oscillations found in $e - N_2$ collisions are not possible in $Ps-N_2$ collisions, and we proceed with calculation of Ps-impact vibrational excitation using the vibrationally-adiabatic approximations in Sec. III. We discuss the results in Sec. IV, and then turn to the Conclusion.

II.   FIXED-NUCLEI SCATTERING CALCULATIONS

In order to calculate the scattering potentials for both $e-N_2$ and $Ps-N_2$ scattering we need the target electron probability density $n(\mathbf{r})$. In the present paper we calculate this quantity from the ground state wavefunctions of Cade et al. [31] at the equilibrium separation $R_e = 2.068$ a.u. as well as at $R =1.85$, 1.95, 2.15 and 2.45 a.u.

For $e-N_2$ scattering we use the static-exchange plus polarization (SEP) approximation as described in [11], using the Hara free electron gas exchange model (HFEGE) [32] and semi-empirical correlation-polarization potential with cutoff of [18]. For $Ps-N_2$ scattering the static potential averages to zero and we use the FEG model of [30] to calculate the exchange and correlation potentials. In both cases we expand the potentials in Legendre polynomials and use the integral equation method of [33] to solve the resulting coupled equations. The calculation at the equilibrium internuclear separation is described in more detail in [6].
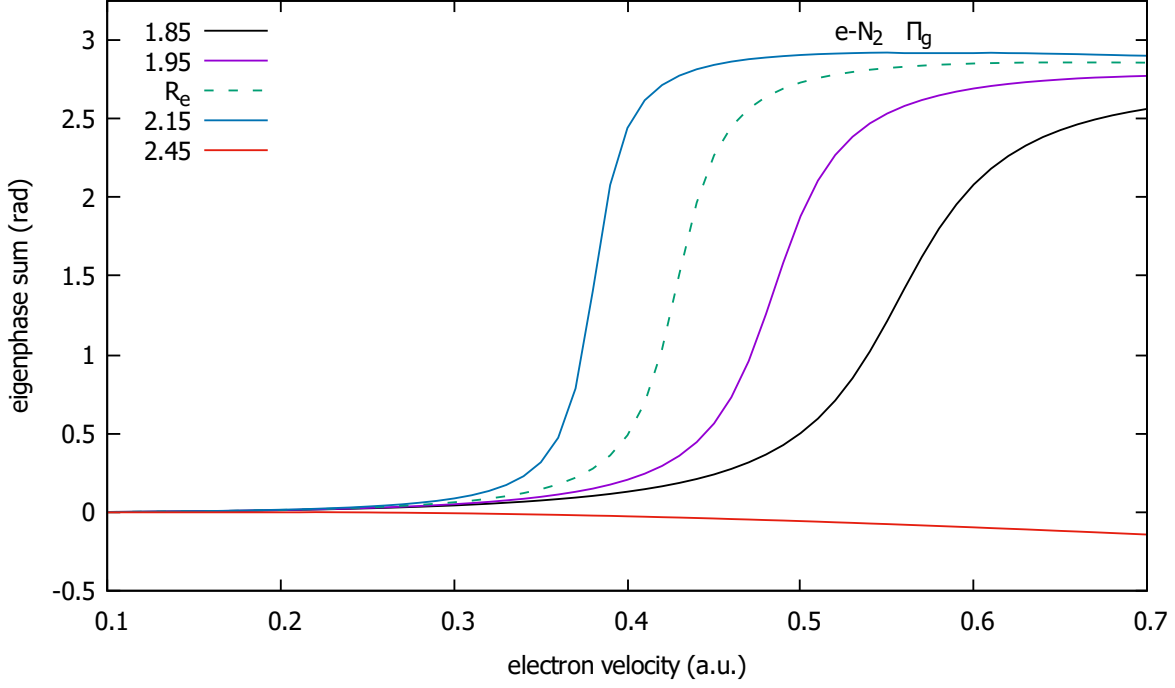
FIG. 1: Eigenphase sums (modulo π) as functions of electron velocity for $e-N_2$ scattering in Π_g symmetry. Curves from bottom to top correspond to increasing internuclear separation R with the exception of the bottom (red) curve corresponding to $R = 2.45$.

In Fig. 1 we present Π_g eigenphase sums for $e-N_2$ scattering as functions of the electron velocity for several internuclear separations with the equilibrium value $R_e = 2.068$ a.u. With the increase of the internuclear separation the resonance width is decreasing and the resonance position moves towards lower energies. In fact in our calculations at $R = 2.45$ a.u. the resonance disappears and becomes a bound state. This is due to an overestimation of the interaction potential since even in the limit $R \to \infty$, corresponding to free N atoms, the actual resonance does not turn into a bound state, but becomes a low-energy $^3P^e$ resonance in $e-N$ scattering [34]. However, the distances about 2.45 a.u. and beyond are too large to affect $e-N_2$ scattering from the ground vibrational state, therefore this inaccuracy is not significant for our purposes. Note that appearance of a bound state increases the absolute value of the eigenphase sum by π at zero energy. However, for plotting convenience the values of eigenphase sums in Fig. 1 are presented modulo π.

In Fig. 2 we present Σ_u eigenphase sums for $Ps-N_2$ scattering as functions of Ps velocity for the same internuclear separations as in the $e-N_2$ case. The eigenphases clearly
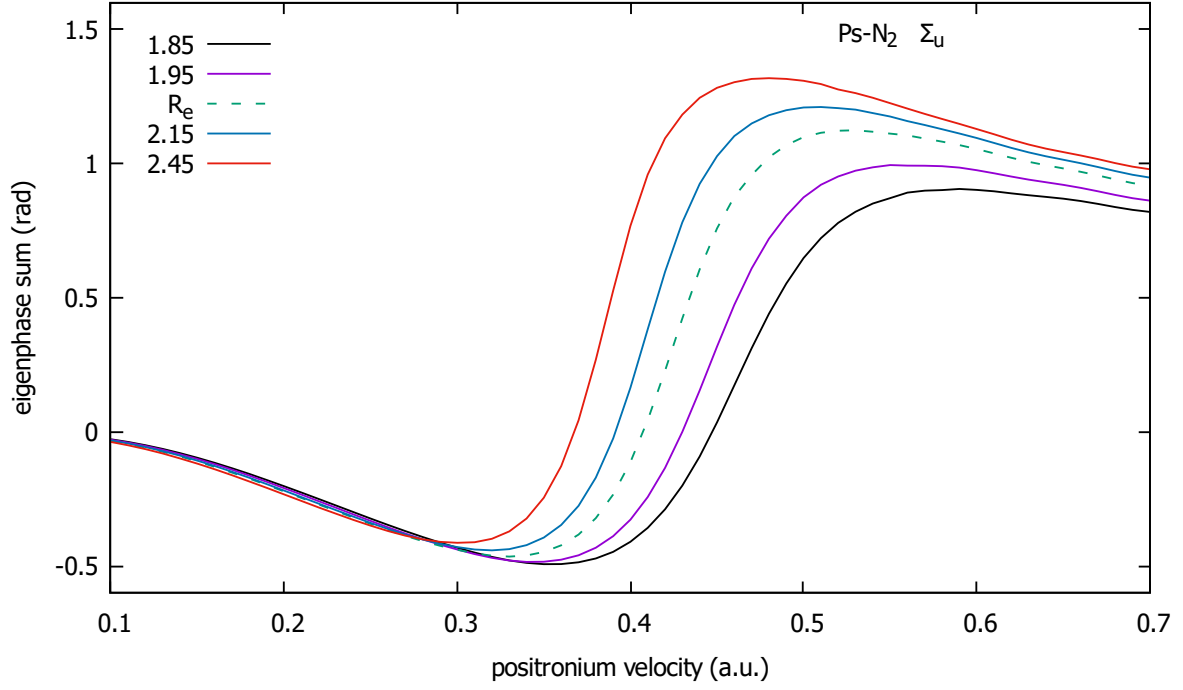
FIG. 2: Eigenphase sums (modulo π) as functions of Ps velocity for Ps-N_2 scattering in Σ_u symmetry. Curves from bottom to top correspond to increasing internuclear separation R.
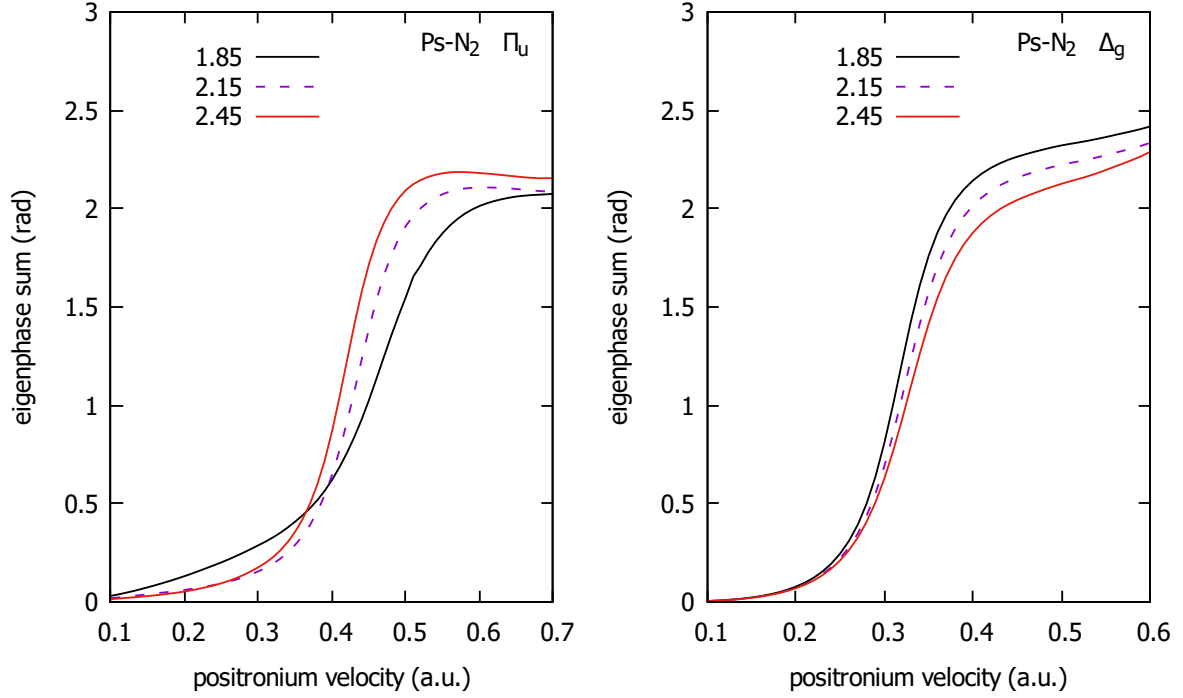

FIG. 3: Eigenphase sums as functions of Ps velocity for Ps-N_2 scattering in Π_u and Δ_g symmetries.

demonstrate the resonance behavior. However, comparison with $e-N_2$ scattering shows two substantial differences. First, there is a substantial background in the Ps case. As a result the eigenphases increase in the resonance region is substantially smaller than in the case of a pure resonance when the phase shift jumps by π, like in the case of electron scattering. Second, the eigenphase sums vary with R much slower in the Ps$-N_2$ case. A similar trend is observed in the Π_u and Δ_g eigenphases shown in Fig. 3. The position of the resonances varies even slower in these symmetries than in the Σ_u case. Moreover, in the Δ_g symmetry the position slightly increases with R.

This is confirmed by calculations of resonance positions and widths for different internuclear distances. The standard procedure [35] was used to obtain these parameters: the eigenphase sum was fitted to the Breit-Wigner formula with a slowly varying background, and the fitting generated the resonance position E_r and the width Γ. In Table I we present resonance parameters for the three resonances found in our calculations. With growing R the positions of Σ_u and Π_u resonances move towards lower energies, but for Δ_g the position is almost independent of R, and in fact is increasing slightly. The physical significance of this will be discussed in section IV.

TABLE I: Resonance position (the first number) and width (the second number) in a.u. for three resonances in Ps-N_2 scattering for five internuclear distances R

R (a.u.)	Σ_u	Π_u	Δ_g
1.85	0.2080/0.1008	0.2217/0.1578	0.09833/0.05605
1.95	0.2018/0.07935	0.2091/0.1380	0.09933/0.05822
2.07	0.1788/0.06892	0.1942/0.1151	0.1006/0.06070
2.15	0.1667/0.06042	0.1879/0.1005	0.1019/0.06325
2.45	0.1500/0.04982	0.1741/0.08366	0.1036/0.07134

The energy position of all three resonances is substantially higher than the energy position of the Π_g resonance in $e-N_2$ scattering, $E_r = 0.0820$ a.u. at equilibrium [24]. However, the velocity positions, $v_r = 0.423$, 0.441, and 0.317 a.u. at $R = R_e$ for Σ_u, Π_u and Δ_g resonances respectively, match pretty well the velocity position, $v_r = 0.42$ a.u. in our calculation ($v_r = 0.405$ according to [24]), of the $e-N_2$ resonance confirming earlier experimental [10] and theoretical [6] data. The energy widths of all resonances are substantially higher than that of

the $e-\mathrm{N}_2$ resonance, $\Gamma = 0.0147$ a.u., and of the vibrational quantum of N_2, $\hbar\omega = 0.010745$ a.u. The velocity widths, in contrast to the velocity position, are also substantially higher than in the $e-\mathrm{N}_2$ case. Therefore we rule out boomerang oscillations and proceed with vibrationally adiabatic calculations of vibrational excitation cross sections.

III. VIBRATIONALLY-ADIABATIC APPROXIMATION

In the vibrationally adiabatic approximation [11] the transition matrix T in the body frame is calculated as

$$T_{LL'}^{vv'} = \int \chi_v(R) T_{LL'}(R) \chi_{v'}(R) dr$$

where L' and L are initial and final projectile angular momenta, v' and v are initial and final vibrational quantum numbers of the target, $\chi_v(R)$ is the vibrational wavefunction, and $T_{LL'}(R)$ is the transition matrix calculated at the fixed internuclear separation R. Assuming fixed orientation of the molecule during the collision, we can calculate then the vibrational excitation cross section as

$$\sigma_{vv'} = \frac{\pi}{k^2} \sum_{LL'} |T_{LL'}^{vv'}|^2$$

where k is the relative momentum.

In Fig. 4 we present three contributions to vibrational excitation cross sections. The Σ_u contribution is dominant, apparently due to the fastest dependence of the resonance parameters on R. For the Δ_g resonance this dependence is the weakest, and the cross section is very small. But even for the dominant Σ_u contribution this dependence is weak as compared to the $e-\mathrm{N}_2$ case when the vibrational excitation cross section for the $v = 1$ state reaches almost 7×10^{-16} cm^2 and for the $v = 2$ state 4.5×10^{-16} cm^2 [24]. Note that in contrast to $e-\mathrm{N}_2$ collisions, in all symmetries for $\mathrm{Ps}-\mathrm{N}_2$ collisions the vibrational excitation drops very fast with v which is another consequence of relatively large resonance widths.

Application of vibrationally adiabatic approximation to elastic $\mathrm{Ps}-\mathrm{N}_2$ scattering shows that inclusion of vibrational motion affects the cross section very little: it is very close to that calculated in the fixed-nuclei approximation at the equilibrium internuclear separation. This is again in contrast to $e-\mathrm{N}_2$ elastic scattering which exhibits boomerang oscillations in the resonance region.

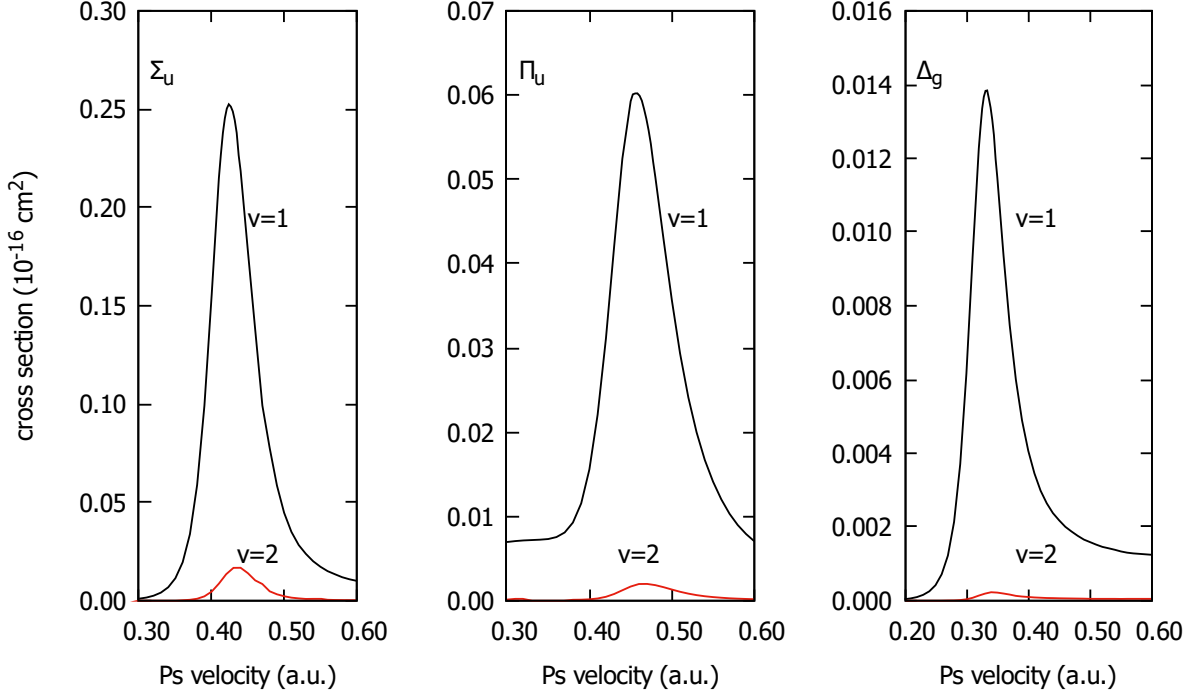FIG. 4: Vibrational excitation of N_2 by Ps impact, three resonance contributions

IV. DISCUSSION

The major difference between fixed-nuclei $e-N_2$ resonance scattering and $Ps-N_2$ resonance scattering is in the dependence of the resonance position and width on R. In the former case it is much stronger resulting in much higher vibrational excitation cross sections. To understand this difference we have investigated the dependence of the interaction potentials on R taking into account the monopole and quadrupole terms in the expansion of the potential in Legendre polynomials

$$V(\mathbf{r}, R) = \sum_{\lambda} V_{\lambda}(r, R) P_{\lambda}(\cos\theta)$$

where θ is the angle between the electron position vector $\mathbf{r}$ and internuclear axis. Averaging this potential over the angular distribution for the resonance of symmetry $\Lambda_{g,u}$, we obtain for the effective projectile-target interaction

$$V_{\text{eff}}(r, R) = \langle L_r \Lambda | V(\mathbf{r}, R) | L_r \Lambda \rangle + \frac{L_r(L_r + 1)}{2mr^2}$$

where L_r is the dominant orbital angular momentum for the resonant state of a given Λ and parity, and m is the mass of the projectile ($m = 1$ a.u. for electron and 2 a.u. for Ps). We
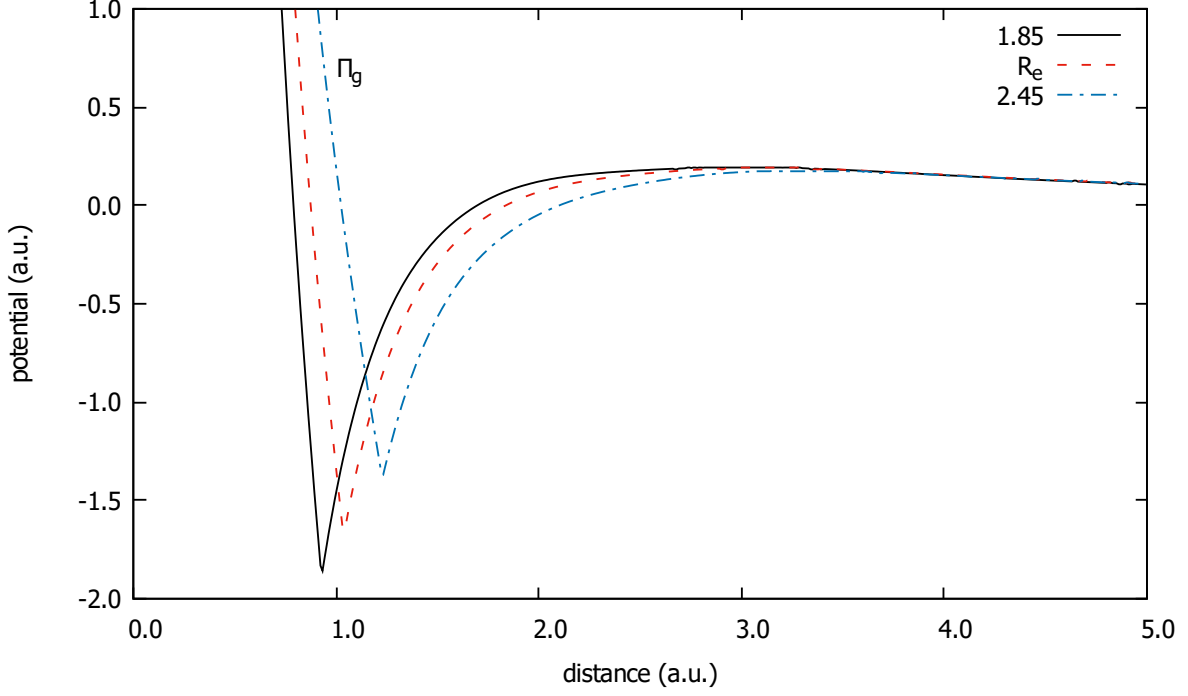
FIG. 5: Effective potentials for $e-N_2$ interaction in Π_g symmetry for several internuclear distances R.

have included the centrifugal term in $V_{\text{eff}}(r, R)$.

In Fig. 5 we present the effective potential for $e-N_2$ interaction in the Π_g symmetry for three values of the internuclear distance. Similar graphs for $Ps-N_2$ interactions in Σ_u and Δ_g symmetries are presented in Fig. 6. The most important range of distances between the projectile and the target, determining positions and widths of low-energy shape resonances, corresponds to that beyond the minima of the potentials. It is apparent that in this range the R dependence of V_{eff} is strongest for the $e-N_2$ interaction. In contrast, the $Ps-N_2$ interaction in the Δ_g symmetry is almost independent of R in the outer range. The R-dependence of the $Ps-N_2$ interaction in the Σ_u symmetry is more noticeable than in the Δ_g case, but still much weaker than that for $e-N_2$. The Π_u case can be placed between Σ_u and Δ_g.

Further analysis shows that such an important difference in R dependence between the $e-N_2$ case and $Ps-N_2$ case is due to the presence of the static potential in the former. Static potential dependence on R is substantially stronger than the R dependence of the exchange and correlation potentials. To understand this, we note that change of R leads to change
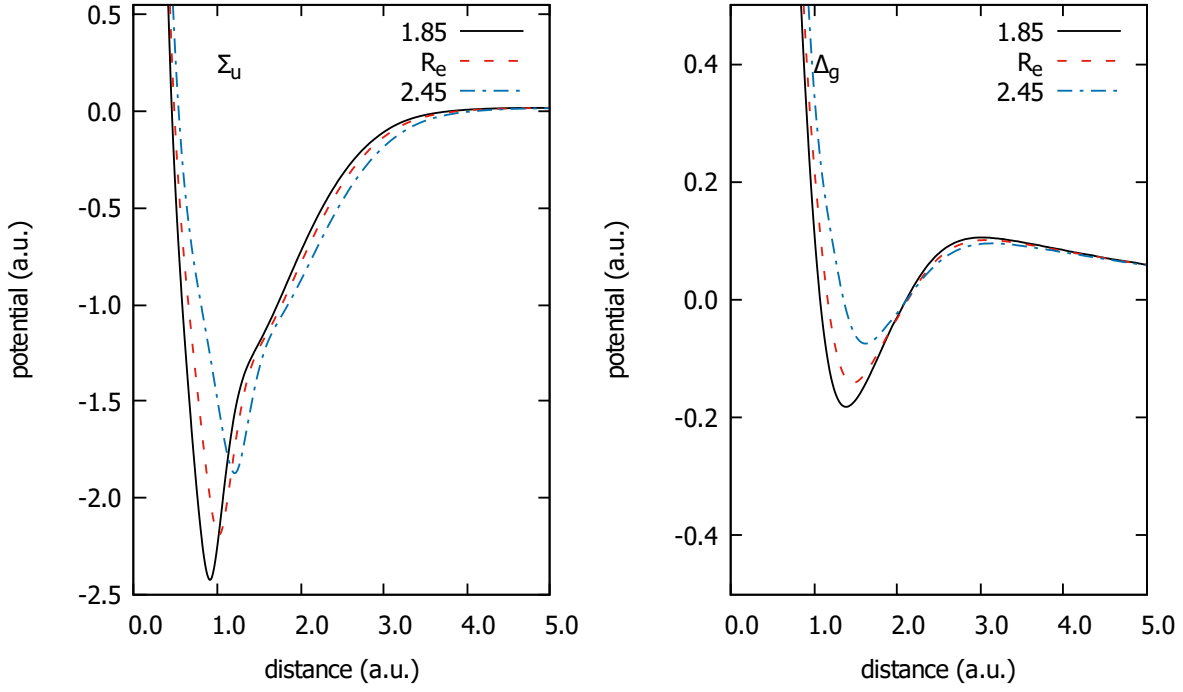
FIG. 6: Effective potentials for Ps-N_2 interaction in Σ_u and Δ_g symmetries.

of target electron probability density $n(\mathbf{r})$, therefore we have to consider the dependence of potentials on $n(\mathbf{r})$. The static potential as a functional of $n(\mathbf{r})$ varies linearly with n. In contrast, the dependence of the exchange potential on n is much weaker. Indeed, in the free-electron-gas model [30, 32] the exchange energy varies with the Fermi momentum k_F as a linear function, or even slower at low k_F [30]. The Fermi momentum is proportional to $n^{1/3}$, therefore the exchange potential varies as $n^{1/3}$ or even slower. The same argument can be put forward for the correlation-polarization potential for $Ps-N_2$ scattering. Moreover, in our model for $e-N_2$ scattering taken from Morrison and Collins [18] the correlation-polarization potential does not depend on R at all.

In spite of the absence of the static contribution to the $Ps-N_2$ interaction, it is strong enough to support resonance states in three symmetries. Comparisons of the $e-N_2$ and $Ps-N_2$ interactions shows that this is due to a relatively large strength of the $Ps-N_2$ exchange potential at small projectile-target distances. To understand this, we compare first the exchange energy of free electron and Ps interactions with a Fermi gas. For the same momentum of projectile the exchange energy in the former case is substantially higher (in absolute magnitude) than the latter because of the positive contribution of positron-electron
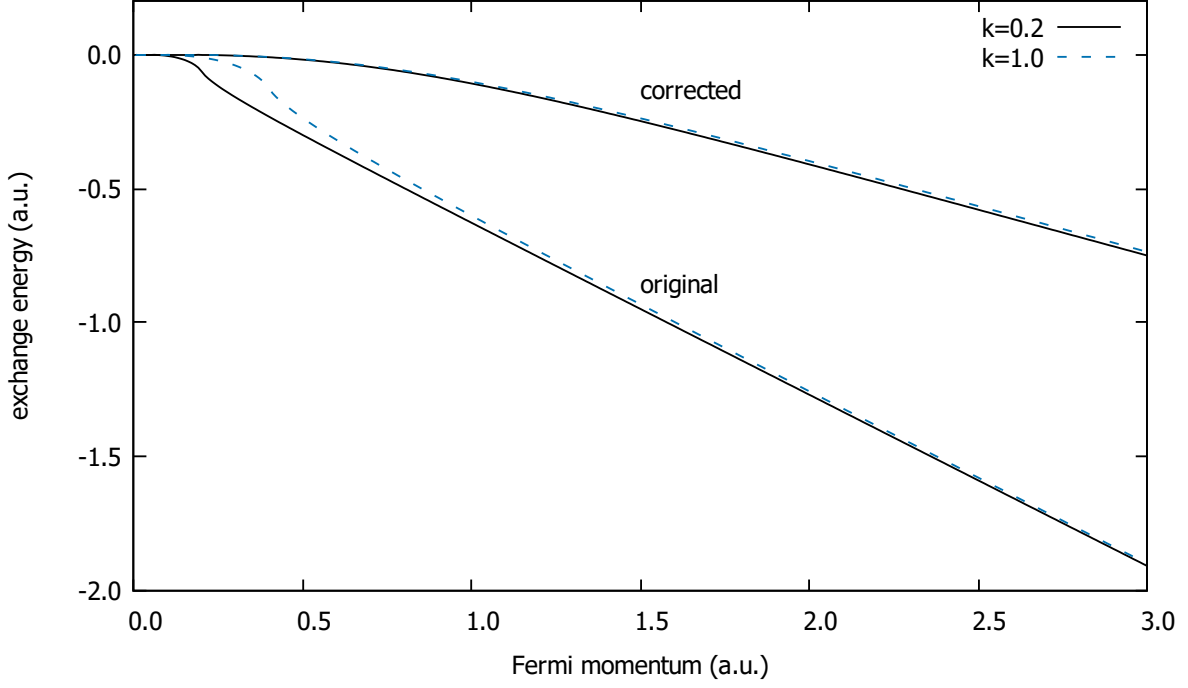
10

FIG. 7: Free-electron gas exchange energy as a function of the Fermi momentum for two projetile electron momenta without and with account of the Hara modification, Eq. (1).

interaction to the exchange energy in the $Ps-N_2$ case [30]. However, the effective electron momentum in the case of $e-N_2$ interaction is substantially higher due to acceleration of the projectile electron when it is penetrating the electron cloud of the target where the nuclear charges are not completely screened. Hara [32] assumed that the kinetic energy E^* of the projectile electron in this region is the same as the target electron energy on the surface of the Fermi sphere, that is

$$E^* = E + E_F + I \tag{1}$$

where E is the electron energy at infinity, E_F is the Fermi energy, and I is the ionization potential. In particular this modification works very well for $e-N_2$ scattering [18]: the cross sections agree with calculations where the exchange is included more accurately [19]. This makes the projectile momentum substantially higher than $(2E)^{1/2}$.

To demonstrate this effect, in Fig. 7 we plot the electron exchange energy with and without modifications of the electron momentum. The modification of the electron momentum substantially reduces (in absolute magnitude) the exchange energy. In contrast, in the case of Ps scattering its momentum changes very little, and the original exchange energy
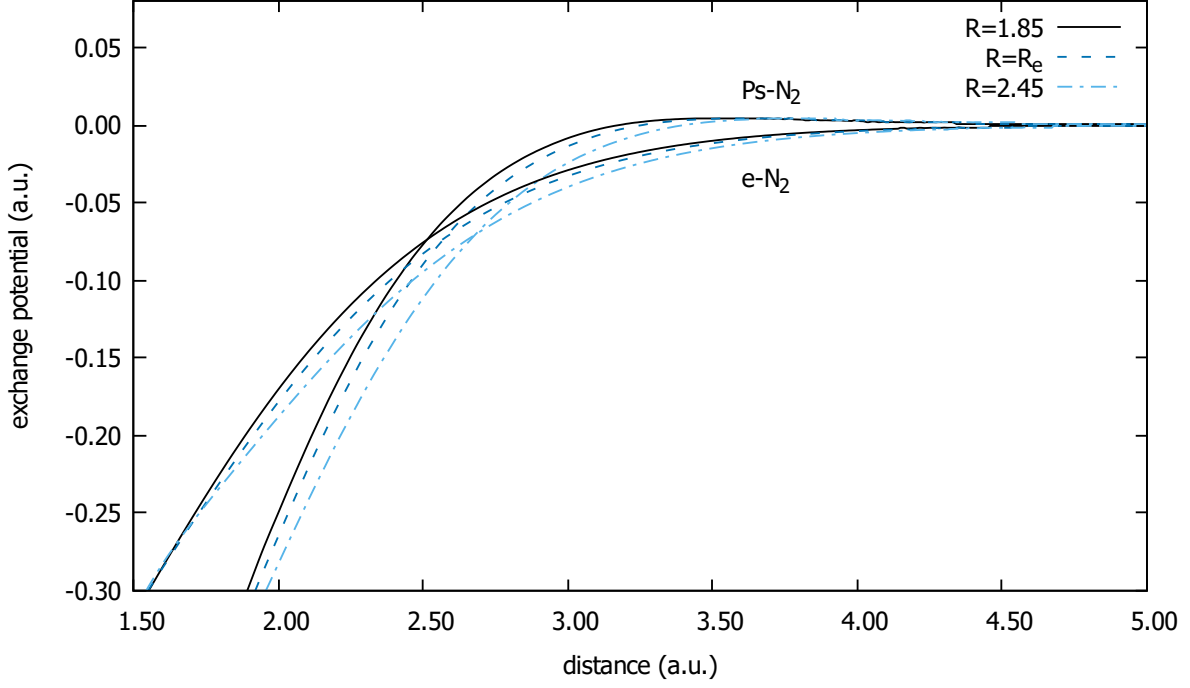
11

FIG. 8: Exchange potentials for $e-N_2$ and Ps-N_2 scattering for three internuclear separations, projectile velocity $v = 0.42$ a.u.

is not modified substantially [30]. In Fig. 8 we compare the exchange potentials for $e-N_2$ and Ps$-N_2$ interactions. At large projectile-target separations the effect of modification of electron momentum is small, and the $e-N_2$ exchange energy is substantially higher (in absolute magnitude) than the Ps$-N_2$ exchange energy. Moreover, the Ps$-N_2$ exchange energy becomes even positive at large distances due to the positron contribution [30]. However, at smaller distances below about 2.5 a.u., the effect of modification of the electron momentum is substantial, and the Ps-N_2 exchange potential becomes larger in absolute magnitude. Physically this means that the electron in Ps remains relatively slow as compared to a free electron, therefore the exchange energy in the Ps case is higher.

V. CONCLUSION

Ps$-N_2$ collisions at the relative velocity about 0.43 a.u. are strongly affected by resonance scattering in Σ_u, Π_u and Δ_g symmetries with the Δ_g resonance producing the largest contribution to the elastic scattering cross section [6]. As a result the calculated total cross

section for Ps$-$N$_2$ collisions [6], plotted as a function of the projectile velocity, looks very similar to the total $e-$N$_2$ cross section which is dominated by the Π_g resonance at the relative collision velocity 0.42 a.u. This confirms experimental observations [9, 10]. However, Ps$-$N$_2$ resonances contribute mostly to the elastic scattering. In the present paper we have shown that the contribution of the vibrational excitation cross section to the total is rather small. This contrasts with $e-$N$_2$ scattering where the peak value of the vibrational excitation cross section is about 7×10^{-16} cm^2, more than an order of magnitude higher than the peak value of the cross section for excitation by Ps impact. Moreover, the width of the resonance in $e-$N$_2$ collisions is substantially lower than in Ps$-$N$_2$ collisions. In the former case the corresponding resonance lifetime is about the same as the vibrational period which leads to the boomerang oscillations in elastic scattering and vibrational excitation [20, 21, 23]. In contrast, in Ps$-$N$_2$ scattering we obtain no oscillations: elastic and vibrational excitation cross sections exhibit just one peak corresponding to the resonance position in the fixed-nuclei approximation.

Our analysis has shown that this difference can be attributed to the difference in potentials for $e-$N$_2$ and Ps$-$N$_2$ interactions. A substantial part of the former is the static interaction which varies relatively fast with the internuclear separation. The static potential is zero for Ps$-$N$_2$ interaction, therefore only exchange and correlation potentials contribute to it. These vary relatively slowly with R because of their weak dependence on the electron probability density. Moreover, because of a relatively large resonance width in Ps$-$N$_2$ scattering, no boomerang oscillations are observed in Ps$-$N$_2$ collision cross sections. This conclusion is relevant also to elastic scattering. The difference in the long-range part of the correlation interaction (polarization for $e-$N$_2$ scattering versus van der Waals for Ps$-$N2 scattering), might be also responsible for the difference between $e-$N$_2$ and Ps$-$N$_2$ resonance scattering.

The calculations performed in the present paper can be improved by a more complete inclusion of the Pauli exclusion principle which can be done either by employing pseudopotentials with repulsive cores [36, 37] or by using the orthogonalizing pseudopotential method [38, 39] which has been successfully employed for treatment of Ps collisions with rare gas atoms [40]. Nevertheless we believe that our conclusions are quite general, and allow us to expect that generally vibrational dynamics in Ps$-$M collisions is not as pronounced as in corresponding $e-$M collisions for a general molecular target M. Indeed, no vibrational structure in Ps collisions with molecules has been observed so far, and no dissociative positronium

attachment channels have been detected. However, experiments on Ps scattering are much more challenging than those on electron scattering, and we do not exclude a possibility of detection of interesting vibrational dynamics for some particular targets in the future.

Acknowledgments

[1] G. Laricchia and H. R. J. Walters, Riv. Nuovo Cimento **35**, 305 (2012).

[2] P. K. Biswas and S. K. Adhikari, J. Phys. B **31**, L737 (1998).

[3] P. K. Biswas and S. K. Adhikari, J. Phys. B **33**, 1575 (2000).

[4] R. S. Wilde and I. I. Fabrikant, Phys. Rev. A **92**, 032708 (2015).

[5] J.-Y. Zhang, M.-S. Wu, Y. Qian, X. Gao, Y.-J. Yang, K. Varga, Z.-C. Yan, and U. Schwingenschlögl Phys. Rev. A **100**, 032701 (2019)

[6] R. S. Wilde and I. I. Fabrikant, Phys. Rev. A **97**, 052708 (2018).

[7] S. J. Brawley, S. Armitage, J. Beale, D. E. Leslie, A. I. Williams, and G. Laricchia, Science **330**, 789 (2010).

[8] S. J. Brawley, A. I. Williams, M. Shipman, and G. Laricchia Phys. Rev. Lett. **105**, 263401 (2010).

[9] S. J. Brawley, A. I. Williams, M. Shipman, and G. Laricchia, J. Phys.: Conf. Series **388**, 012018 (2012).

[10] M. Shipman, S. J. Brawley, L. Sarkadi, and G. Laricchia, Phys. Rev. A **95**, 032704 (2017).

[11] N. F. Lane, Rev. Mod. Phys. **52**, 29 (1980).

[12] H. Hotop, M.-W. Ruf, M. Allan, and I. I. Fabrikant, Adv. At. Mol. Phys. **49**, 85 (2003).

[13] I. I. Fabrikant, S. Eden, N. J. Mason and J. Fedor, Adv. At. Mol. Opt. Phys. **66**, 546 (2017).

[14] P. G. Burke and A.-L. Sinfailam, J. Phys. B **3**, 641 (1970).

[15] P. G. Burke and N. Chandra, J. Phys. B **5**, 1696 (1972).

[16] M. A. Morrison and B. I. Schneider, Phys. Rev. A **16**, 1003 (1977).

[17] B. D. Buckley and P. G. Burke, J. Phys. B **10**, 725 (1977).

[18] M. A. Morrison and L. A. Collins, Phys. Rev. A **17**, 918 (1978).

[19] B. I. Schneider, Phys. Rev. A **24**, 1 (1981).

[20] A. Herzenberg, J. Phys. B **1**, 548 (1968).

[21] D. T. Birtwistle and A. Herzenberg, J. Phys. B **4**, 53 (1971).

[22] N. Chandra and A. Temkin, Phys. Rev. A **13**, 188 (1976).

[23] B. I. Schneider, M. Le Dourneuf, and Vo Ky Lan, Phys. Rev. Lett. **43**, 1926 (1979).

[24] A. U. Hazi, T. N. Rescigno, and M. Kurilla, Phys. Rev. A **23**, 1089 (1981).

[25] W. Sun, M. A. Morrison, W. A. Isaacs, W. K. Trail, D. T. Alle, R. J. Gulley, M. J. Brennan, and S. J. Buckman, Phys. Rev. A **52**, 1229 (1995).

[26] H. Feng, W. Sun, and M. A. Morrison, Phys. Rev. A **68**, 062709 (2003).

[27] K. R. Hoffman, M. S. Dababneh, Y. F. Hsieh, W. E. Kauppila, V. Pol, J. H. Smart, and T. S. Stein, Phys. Rev. A **25**, 1393 (1982).

[28] B. K. Elza, T. L. Gibson, M. A. Morrison, and B. C. Saha, J. Phys. B: At. Mol. Phys. **22**, 113 (1989).

[29] G. F. Gribakin, J. A. Young, and C. M. Surko, Rev. Mod. Phys. **82**, 2557 (2010).

[30] I. I. Fabrikant and R. S. Wilde, Phys. Rev. A **97**, 052707 (2018).

[31] P. E. Cade, K. D. Sales, and A. C. Wahl, J. Chem. Phys. **44**, 1973 (1966).

[32] S. Hara, J. Phys. Soc. Japan **22**, 710 (1967).

[33] M. A. Morrison, in *Electron-Molecule and Photon-Molecule Collisions*, eds. T. Rescigno, V. McKoy and B. Schneider (Plenum Press, New York 1979), p. 15.

[34] C. A. Ramsbottom and K. L. Bell, Phys. Scr. **50**, 666 (1994).

[35] A. U. Hazi, Phys. Rev. A **19**, 920 (1979).

[36] I. I. Fabrikant and G. F. Gribakin, Phys. Rev. A **90**, 052717 (2014); *ibid.* **97**, 019903(E) (2018).

[37] G. F. Gribakin, A. R. Swann, R. S. Wilde, and I. I. Fabrikant, J. Phys. B **49**, 064004 (2016).

[38] J. Mitroy and G. G. Ryzhikh, Comput. Phys. Commun. **123**, 103 (1999).

[39] I. A. Ivanov, M. W. J. Bromley, and J. Mitroy, Comp. Phys. Comm. **152**, 9 (2003).

[40] R. S. Wilde and I. I. Fabrikant, Phys. Rev. A **98**, 042703 (2018).